Pergamon

Cement and Concrete Research 33 (2003) 769–774

CEMENT AND CONCRETE RESEARCH

Communication

^{29}Si and ^{27}Al NMR study of alkali-activated slag

Shao-Dong Wang[a], Karen L. Scrivener[b,*]

[a]*Materials Institute, Chongqing Jianzhu University, Campus B, Chongqing 400045, China*
[b]*Laboratory of Construction Materials, École Polytechnique Fédérale de Lausanne, 1015 Lausanne, Switzerland*

Received 1 September 1999; accepted 17 October 2002

Abstract

This paper presents the results of the investigation of the hydration of alkali-activated slag (AAS) by nuclear magnetic resonance spectroscopy (NMR). The cross-polarization (CP) technique was used in combination with magic-angle spinning (MAS). This research was part of a systematic study of alkaline activation of slag by several different techniques, including X-ray diffraction (XRD), scanning electron microscopy (SEM) coupled with X-ray microanalysis of energy dispersive spectra (EDS), differential thermal analysis (DTA) and calorimetry. This NMR study provides information on the polymerization of silicates, the role of aluminates in cement hydration and the nanostructure of C–S–H gel.

Keywords: Alkali-activated slag; NMR; C–S–H; Microstructure; EDX

1. Introduction

Blast furnace slag is produced from the manufacture of pig iron. If the molten slag is quenched sufficiently rapidly, it forms a material in which the principal component is a calcium-magnesium alumino-silicate glass. The quenched ground product is known as ground granulated blast furnace slag (GGBS) and is widely used as a supplementary cementitious material in Portland cement concrete. Slag has latent hydraulic properties; Portland cement, lime and gypsum are common activators. The activation of slag with alkaline liquids (e.g., NaOH or water glass) is a relatively new approach that was first developed in Ukraine [1–4], but only started to receive worldwide attention about 15 years ago [5–8].

Nuclear magnetic resonance spectroscopy (NMR) gives detailed structural information on materials containing atoms, which possess a magnetic moment, e.g., ^{1}H, ^{13}C, ^{27}Al, ^{29}Si and ^{31}P. In particular, solid state ^{29}Si NMR using magic-angle spinning (MAS) has proved useful in the structural characterization of silicates. The different chemical shifts in spectra are normally interpreted in terms of the different silicon Q_n environments, where n denotes the number of bridging oxygen linked to other Si atoms for each Q (SiO_4) unit. Thus, Q_0 are Si in orthosilicate groups (discrete tetrahedra SiO_4), Q_1 are Si in dimers and as chain end tetrahedra of higher polymers and Q_2 for middle groups such as those underlined in pentamers (Si–Si–Si–Si–Si, where oxygen are omitted) and higher polymers. The ^{29}Si chemical shift is also affected by the presence of aluminum in the first coordination shell and Q_2(1A1) is used to denote the Si underlined in Si–Si–Al–Si–Si groups [9,10]. Likewise, the term Q_2(0A1) is sometimes used to emphasize that the Q_2 has no aluminum in the first coordination shell.

1.1. Structural models of C–S–H

In 1986 and 1993, Taylor [11,12] proposed a disordered layer structure for C–S–H gel, in which most of the layers were structurally imperfect ones of jennite and others are similarly related to 1.4 nm tobermorite. Silicates in jennite and 1.4 nm tobermorite are long chains, but those in C–S–H are finite chains of dreierketten structure, i.e., they are linked in such a way as to repeat at an interval of three tetrahedra. Every third tetrahedron is a bridging tetrahedron and these are the ones that may be absent, accounting for the chain lengths of 2, 5, 8, . . ., $3n - 1$ observed experimentally.

Al substitution for Si is confined to the bridging tetrahedron. It is also possible that AFm type layers may be intermixed with those of C–S–H at various scales, ranging

* Corresponding author. Tel.: +41-21-693-5843; fax: +41-21-693-5800.
E-mail address: karen.scrivener@epfl.ch (K.L. Scrivener).

0008-8846/02/$ – see front matter © 2002 Published by Elsevier Science Ltd.
doi:10.1016/S0008-8846(02)01044-X

from single layers to microcrystals sufficiently large to be detected by XRD. This supposition is supported by the fact that the main layers of AFm phases have net positive charges and those of C–S–H have net negative charges. Hydrotalcite-type phases and CH also contain positively charged main layers and might be expected to behave similarly. Such intercalcation may explain some of the foreign ions such as Al^{3+}, Mg^{2+} and SO_4^{2-} detected in microanalysis of C–S–H gel in the scanning electron microscopy (SEM).

In 1992 and 1993, Richardson and Groves [13,14] proposed a similar model, which attempts to fit a wider range of chemical compositions and to combine two proposed approaches, i.e., jennite/tobermorite- and tobermorite/CH-based structures. To a large extent, Richardson and Groves model can be considered as a mathematical expression of Taylor's model. While both models agree that any Al substitution for Si must be limited to bridging Si tetrahedra, the extent to which this can occur is considered small (Al/Ca = 0.02) by Taylor but large (Al/Si = 0.22) by Richardson and Groves. However, this apparent contradiction is primarily due to the different global compositions of the systems considered.

1.2. Hydration products of AAS pastes

In recent work, using backscattered electron imaging combined with EDS X-ray microanalysis, XRD and DTA, poorly crystalline C–S–H(I) with a C/S ratio of 1.0–1.2 was found to be the major hydration product of AAS pastes activated with NaOH and waterglass [7,8]. Hydrotalcite and an AFm-type phase (close to C_4AH_{13}) may be also present depending on the composition of slag, the type of activator and the curing conditions. The hydrogarnet katoite was found as a hydration product at high temperatures [6].

The C–S–H gel was found to contain a substantial amount of Al (Al/Si around 0.2 ± 0.02). This solid state NMR study was designed to understand if the aluminum is in solid solution replacing Si tetrahedra or in AFm layers intermixed with C–S–H and to obtain additional information into the nanostructure of C–S–H.

2. Experimental

2.1. Materials

A British slag was used, supplied by the Appleby Group. Its chemical composition and atomic ratios are given in Table 1. A small amount of merwinite and a trace of gehlenite were present. The specific surface area was 4100 cm^2/g (Blaine). Alkaline solutions of sodium hydroxide and waterglass (wg) having a SiO_2/Na_2O ratio (i.e., modulus) of 1.0 were made from reagent grade chemicals, with compositions in grams per 100 milliliters given in Table 2.

Table 1
Chemical compositions and atomic ratios of the slag used

SiO_2	Al_2O_3	CaO	MgO	Fe_2O_3	MnO	TiO_2	Total	Al/Si	Ca/Si	Mg/Si
35.5	12.5	40.2	9.0	0.6	0.5	0.7	99.1	0.41	1.21	0.38

Table 2
Composition of alkaline solutions (g/100 ml)

Notation *	Formula	Na_2O	SiO_2	Total solid	pH
4 M NaOH	NaOH	12.4	0	12.4	14.6
2 M wg (1 m)	$Na_2O{\cdot}SiO_2$	12.4	12.0	24.4	13.4

Where M = concentration in mol/ml, wg = waterglass and m = SiO_2/Na_2O, i.e., modulus of waterglass.

2.2. Sample preparation

Ground slag was mixed with alkaline solutions with liquid/solid ratio of 0.25 (volume of solution in milliliters:

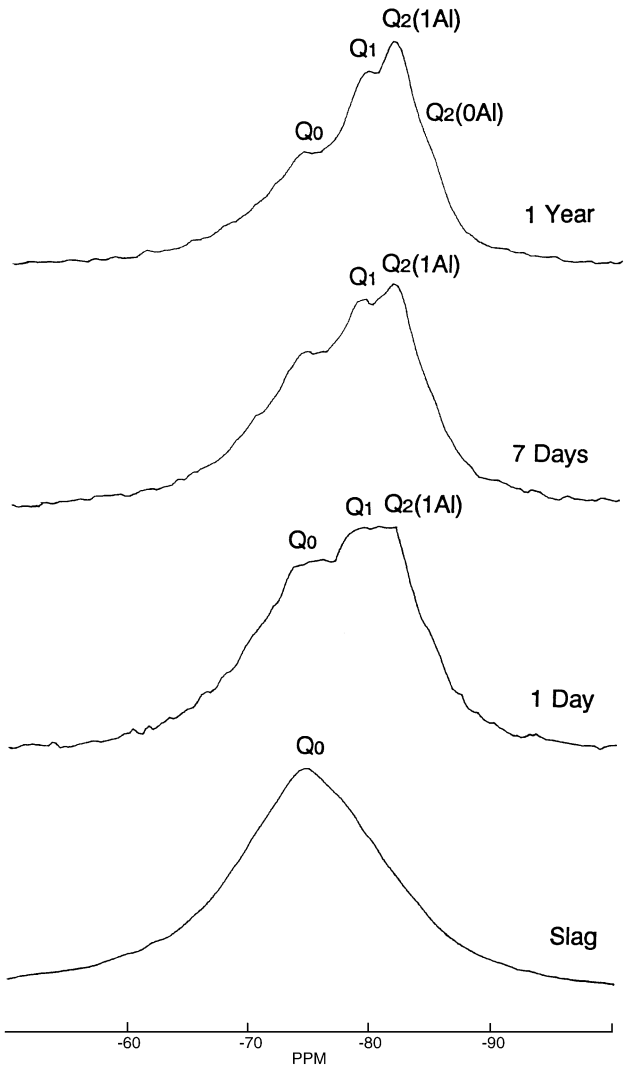

Fig. 1. ^{29}Si MAS NMR spectra for slag activated with 4 M NaOH at from 1 day to 1 year.

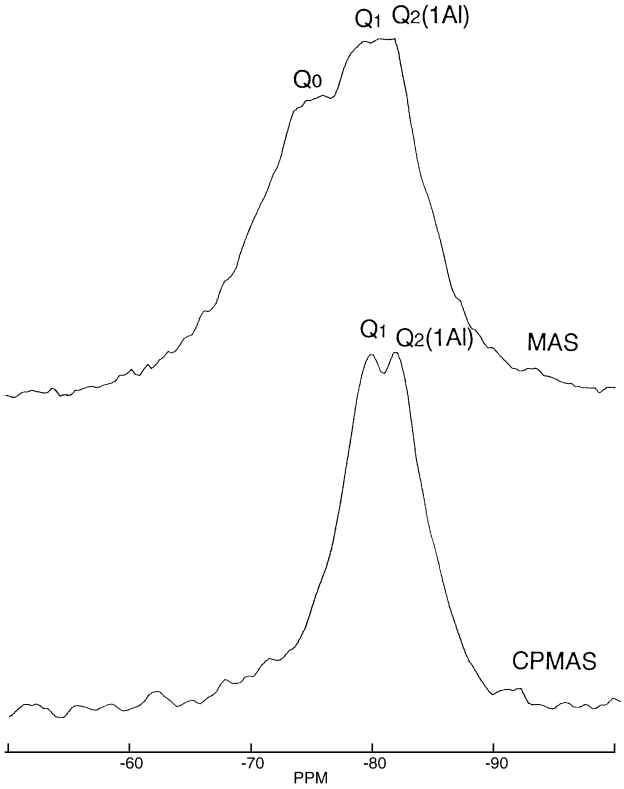

Fig. 2. ^{29}Si CPMAS and MAS NMR spectra for slag activated with 4 M NaOH at 1 day.

weight of slag in grams). The mixes were cast into plastic sample bottles, sealed and cured at either 20 or 80 ± 2 °C. At the required ages, hydration was stopped by freezing in a mixture of solid CO_2 and methanol (− 80 °C). The samples were then freeze-dried. Dry samples were ground in an agate mortar to a fine powder for NMR examination.

2.3. Solid state NMR spectroscopy

Solid-state NMR spectra were recorded on a Bruker MSL-300 spectrometer equipped with a 7.0-T magnet in which the resonance frequencies for ^{29}Si and ^{27}Al are 59.63 and 78.21 MHz, respectively. High-power proton decoupling was used for both ^{29}Si and ^{27}Al spectra, and chemical shifts are quoted relative to external tetramethylsilane (TMS) for ^{29}Si, and to 1 M aqueous aluminum nitrate solution for ^{27}Al. Typical acquisition parameters for recording the ^{29}Si spectra were 4.5-kHz sample spinning speed, 2.5-s pulse length and a 2-s repetition time between scans. ^{29}Si CPMAS experiments were performed using a contact time of 0.5 ms and a recycle delay of 0.5 s. ^{27}Al spectra were recorded using approximately 10-kHz spinning speed, 0.6-s pulse lengths with a recycle delay of 0.5 s between scans.

The spectra are plotted on an arbitrary height scale relative to the strongest peak in the spectra so absolute peak heights cannot be compared for different spectra.

3. Results and discussion

3.1. NaOH-activated system at 20 °C

Fig. 1 shows ^{29}Si MAS NMR spectra for slag activated with 4 M NaOH at 1 day, 7 days and 1 year. Figs. 2 and 3 compare ^{29}Si CPMAS and ^{29}Si NMR spectra at 1 and 7 days. These spectra contain similar features to those observed by Richardson et al. [10] on similar samples after hydration at 60 °C for 1 week. For all ages, three main peaks, at − 74 ± 0.4 ppm for Q_0 sites from unhydrated slag, − 78.8 ± 0.7 ppm for Q_1 sites and − 81.5 ± 0.5 ppm for Q_2(1Al) sites can be detected. The presence of a strong peak for Q_2(1Al) sites, together with the absence of Q_1(1Al) sites (which is expected to resonate between − 75 and − 76 ppm), supports the model of dreierketten chains with isomorphous replacement of bridging silicon by aluminum [15]. However, the presence of the presence of a shoulder Q_2(0Al) indicates that there are also Si ions occupying these bridging positions. These findings are consistent with the

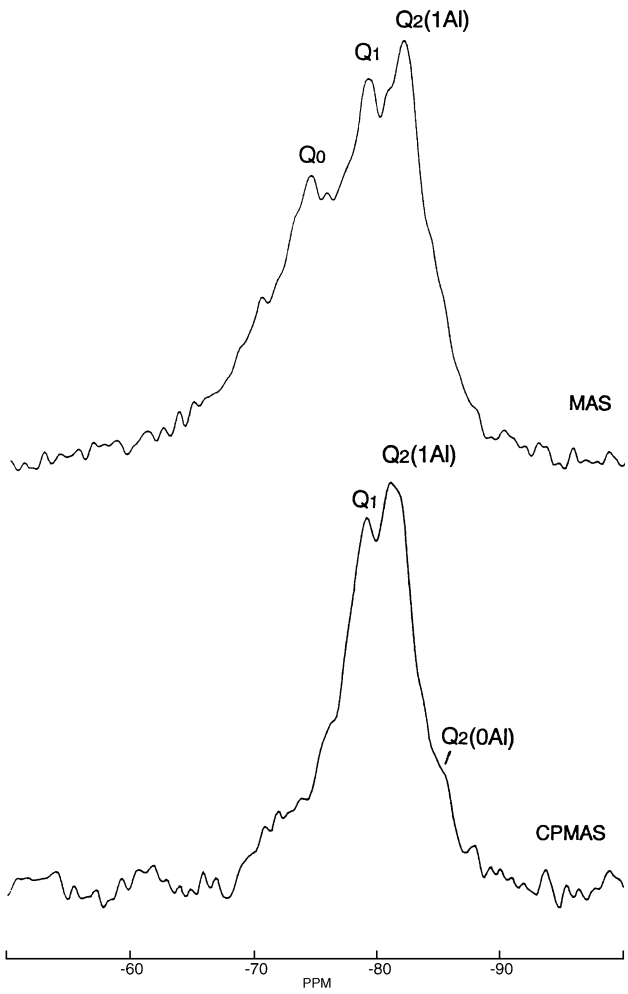

Fig. 3. ^{29}Si CPMAS and MAS NMR spectra for slag activated with 4 M NaOH at 7 days.

Table 3
Atomic ratios from EDS X-ray microanalysis in the SEM for C–S–H gels formed in different conditions [6]

Alkalis	Waterglass		NaOH		
Curing T	20 °C		20 °C		80 °C
Age	1–7 days	1 year	1–7 days	1 year	6 months
Ca/Si of CSH	1.0	1.0	1.1	1.1	1.1
Al/Si of CSH	0.20	0.21	0.18	0.20	0.20

data from EDS microanalysis. Assuming that pentameric chains predominate, the presence of Al in all the bridging sites would result in an Al/Si ratio of 0.25 but the measured Al/Si ratios are around 0.2 (see Table 3 below). It is difficult to be more quantitative about the relative amounts of the different Q_n species due to the amount of peak overlap. This is a consequence partly of the range of environments present (as in amorphous material) resulting in a chemical shift dispersion and partly of broadening due to interactions with unpaired electrons from paramagnetic components in the slag (such as iron). Nevertheless, the height of the Q_2(1Al) peak relative to the Q_1 peak and the increasing strength of the Q_2(0Al) peak suggest:

1. All the aluminum detected in the C–S–H by EDS X-ray microanalysis is incorporated in the silicate chains in bridging sites.
2. The chains are at least pentamers and octametric and longer length chains form at later ages.
3. Initially, the incorporation of aluminum in the bridging sites seems to be preferred, with silicon being incorporated later.

Although the overall Al/Si ratio in the slag is 0.41, a considerable amount of Al is combined with the magnesium in hydrotalcite and, in the NaOH-activated pastes, as an AFm phase. Approximate calculation based on the magnesium content of the slag, the Al/Mg ratio of the hydrotalcite, the calcium content and the Ca/Si ratio of the C–S–H indicate that about half the aluminum is combined in these phases, if all the remaining aluminum is combined in the C–S–H the Al/Si ratio would be about 0.2, which corresponds to the value measured by EDS X-ray microanalysis at later ages. This, taken alongside the evidence that Al is incorporated into bridging sites before silicon suggests that the Al/Si ratio observed is limited more by the amount of Al available than by any intrinsic limit to substitution.

Fig. 4 shows NMR spectra of ^{27}Al CPMAS and MAS for slag activated with 4 M NaOH at 1 day. It can been seen that

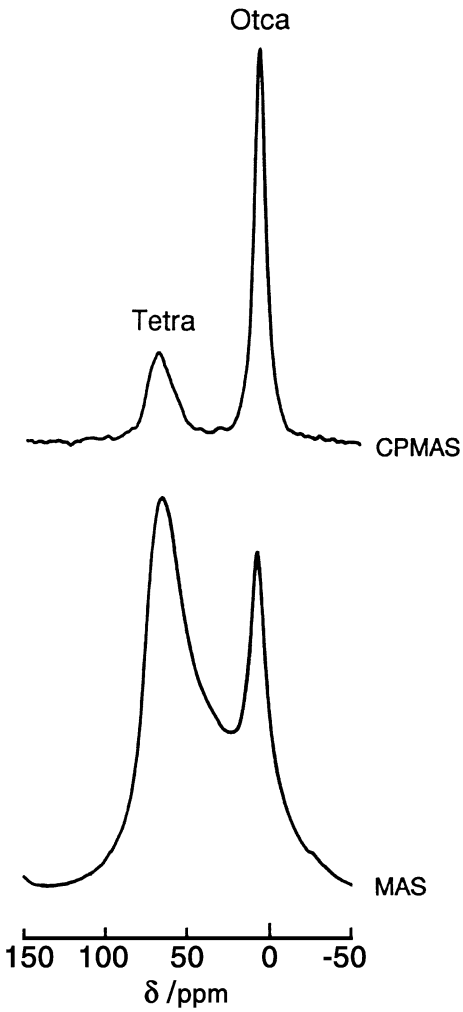

Fig. 4. ^{27}Al CPMAS and MAS NMR spectra for slag activated with 4 M NaOH at 1 day.

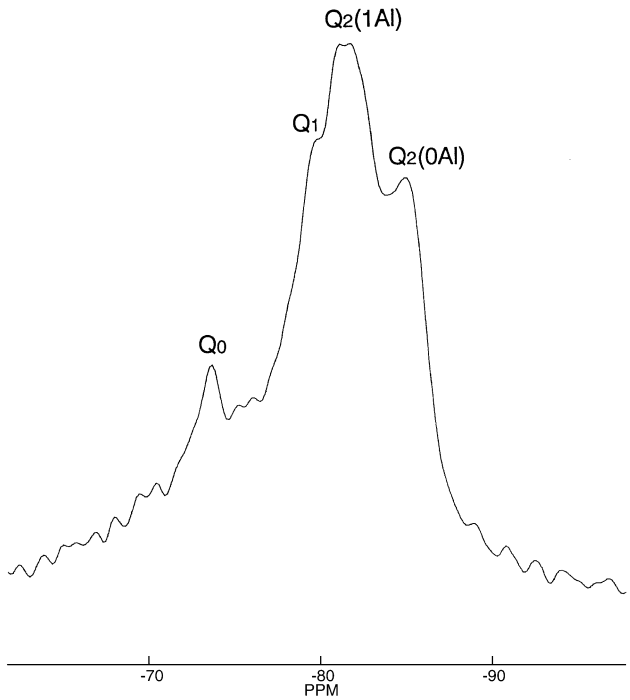

Fig. 5. ^{29}Si MAS NMR spectrum for slag activated with 4 M NaOH cured at 80 °C for 6 months.

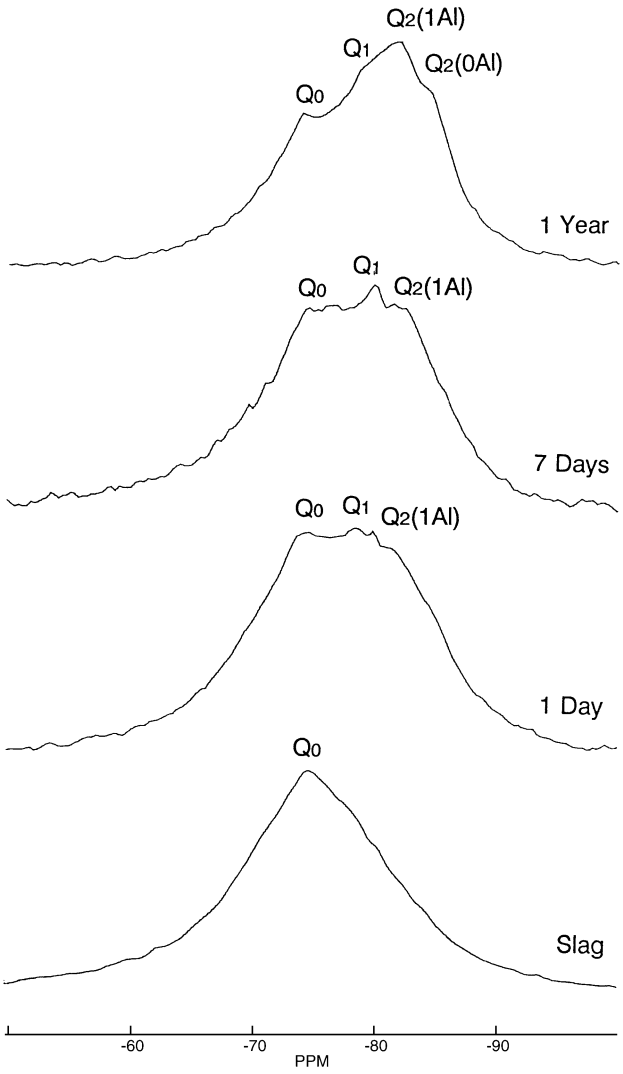

Fig. 6. ^{29}Si MAS NMR spectra for slag activated with 2 M wg (1 m) at from 1 day to 1 year.

4-coordinated (tetrahedral) and 6-coordinated (octahedral) aluminum can be clearly distinguished from each other. In the upper cross-polarised spectrum, the signal for the tetrahedral Al in the slag glass in minimal and the spectrum shows peaks from aluminum in tetrahedral coordination in the C–S–H and in octahedral coordination in hydrotalcite and in AFm. The tetrahedral peak is significantly broader, corresponding to the lower degree of crystallinity of the C–S–H phase. Given the different peak widths, it is difficult to draw any conclusions about the relative amounts of aluminum in the two sites. However, as discussed above, EDS microanalysis and the bulk chemistry of the system suggest that there are approximately equal quantities in the two different coordinations.

3.2. NaOH-activated system at 80 °C

Fig. 5 shows a NMR spectrum of ^{29}Si MAS for slag activated with 4 M NaOH cured at 80 °C for 6 months. Comparing this spectrum with that from the same system hydrated at 20 °C for 1 year. It is apparent that the peaks are much sharper, corresponding to a higher degree of crystallinity of the C–S–H phase, as also observed by X-ray diffraction (XRD) [6]. Again, this difference in peak width makes it difficult to draw further conclusions from the relative heights of the peaks. However, the predominance of the Q_2 peaks (1Al and 0Al) relative to the Q_1 peak suggest a longer average chain length for the C–S–H than at 20 °C.

3.3. Waterglass-activated system at 20 °C

Fig. 6 shows NMR spectra of ^{29}Si MAS for slag activated with 2 M wg (1 m) at 1 day, 7 days and 1 year. These ^{29}Si NMR spectra are similar to those for slag activated with NaOH but in this case the peaks are broader, suggesting a lower degree of crystallinity of the C–S–H compared to the NaOH-activated system. Despite the broader and more overlapped peaks, the Q_2(0Al) peaks seem to be stronger relative to the Q_2(1Al) peaks than in

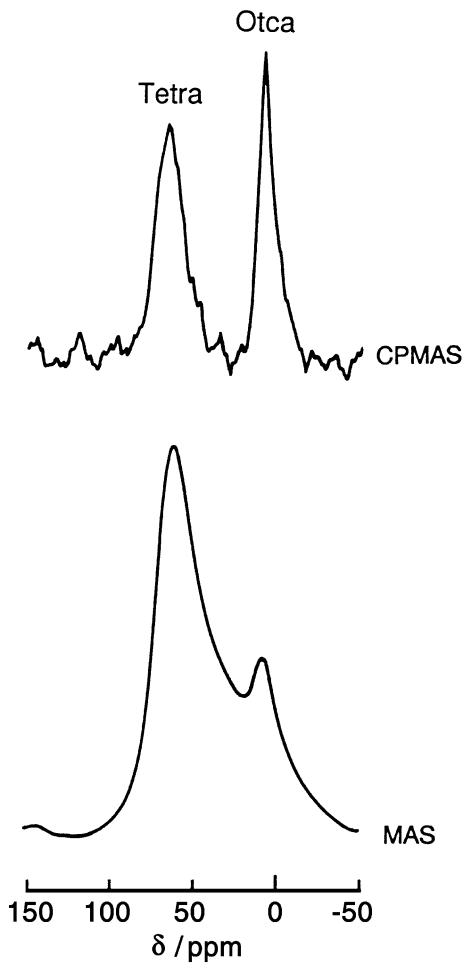

Fig. 7. ^{27}Al CPMAS and MAS NMR spectra for slag activated with 2 M wg (1 m) at 1 day.

the NaOH-activated system. These differences may be attributed to the effect of waterglass. Waterglass solution with a modulus of 1 is known to consist mainly of discrete tetrahedra SiO_4 [16]. Discrete orthosilicate group would be expected to be more available to form bridging tetrahedra.

Fig. 7 shows NMR spectra of ^{27}Al CPMAS and MAS for slag activated with 2 M wg (1 m) at 1 day. Similar to the case of slag activated with NaOH, both 4-coordinate aluminum and 6-coordinate aluminum are detected, but the relative quantity of 4-coordinate aluminum is larger in this case. As slag activated with waterglass was found to form no AFm [6], the 6-coordinate aluminum comes only from hydrotalcite. The hydrotalcite was identified as tiny crystals being closely mixed with C–S–H gel [6].

4. General discussion

The present work has identified that aluminum may be incorporated in the bridging sites of silicate chains in C–S–H even in very young pastes.

For C_3S pastes cured at 25 °C, calculations based on ^{29}Si MAS NMR data gave mean chain lengths of 2.1, 2.6, 3.3 and 4.8 for 1 day, 1 month, 1 year and 26 years, respectively [12]. Even though precis data are not available from this NMR study, it is apparent that the chain length is much higher in the case of alkali-activated slags (AAS). Also, Richardson et al. [10] obtained a mean chain length of 4.83 for a similar slag activated with 5 M KOH cured at 60 °C for 1 week. Although there may be other factors, it can be suggested that the availability of monomeric species such as $Al(OH)_4^-$ or of silicate monomers in the waterglass activated system facilitate the polymerisation of the silicate chains in C–S–H. In the NaOH-activated system, where monomeric silicate is not readily available, a clear preference for the incorporation of aluminum in the bridging sites is seen.

It is also apparent that the amount of aluminum available to enter the C–S–H structure in AAS systems is that remaining after it has been combined with magnesium in a hydrotalcite type phase or with ‘excess’ calcium in AFm phases. (The question remains and will not be discussed further here, as to why the Ca/Si ratio of C–S–H appears to be limited to about 1.1 in AAS systems, with excess calcium forming an AFm phase, rather than increasing the Ca/Si ratio as in Portland cement pastes). Nevertheless, the superabundance of calcium and of other species which can combine with aluminum in other phases (AFm and ettringite-related AFt phases) probably explains the lower Al/Si ratios of C–S–H in Portland cement systems.

5. Conclusions

This NMR study shows that aluminum is incorporated into the silicate chains of C–S–H formed in AAS systems. This incorporation, even at early ages, is associated with a longer chain length of the C–S–H than in C_3S or Portland cement systems.

The NMR study also confirms the increase in C–S–H crystallinity with higher curing temperatures and its decrease in crystallinity in waterglass-activated systems relative to NaOH-activated systems.

Acknowledgements

The first author is grateful to The Institution of Mining and Metallurgy, UK for the award of a Stanley Elmore Fellowship and to The Committee of Vice Chancellors and Principals and Imperial College for the award of an Overseas Research Studentship. Thanks to the University of London Intercollegiate Research Services for provision of the solid state NMR facility, to Dr. P.J. Barrie for his help in the interpretation of the NMR results and to Professor H.F.W. Taylor for his help throughout the work.

References

[1] V.D. Glukhovsky, Ancient, modern and future concretes, 1st Int. Conf. Alkaline Cem. Concr. Kiev. 1 (1994) 1–9.
[2] P.V. Krivenko, Alkaline cements, 1st Int. Conf. Alkaline Cem. Concr. Kiev. 1 (1994) 11–129.
[3] P.V. Krivenko, Alkaline cements, 9th Int. Congr. Chem. Cem., New Delhi, 4 (1992) 482–488.
[4] V.D. Glukhovsky, G.S. Rostovskaja, G.V. Rumyna, High strength slag-alkaline cements, 7th Int. Congr. Chem. Cem., Paris 3 (1980) V164–V168.
[5] B. Talling, J. Brandstetr, Present state and future of alkali-activated slag concretes, 3rd Int. Conf. Fly Ash, Silica Fume, Slag and Natural Pozzolans in Concrete, Trondheim, 2 (1989) 1519–1546.
[6] S.D. Wang, Alkaline activation of slag, PhD thesis of the University of London, Imperial College, 1995.
[7] S.D. Wang, K.L. Scrivener, A study of the microchemistry of alkaline activation of slag, 3rd Beijing Int. Symp. Cem. Concr., Beijing, 2 (1993) 1047–1053.
[8] S.D. Wang, K.L. Scrivener, Hydration products of alkali activated slag, Cem. Concr. Res. 25 (3) (1995) 561–571.
[9] R.J. Kirkpatrick, MAS NMR spectroscopy of minerals and glasses, Rev. Miner. 18 (1998) 341–403.
[10] I.G. Richardson, A.R. Brough, R. Brydson, C.M. Dobson, G.W. Groves, Location of aluminum in substituted calcium silicate hydrate (C–S–H) gels as determined by ^{29}Si and ^{27}Al NMR and EELS, J. Am. Ceram. Soc. 76 (9) (1993) 2285–2288.
[11] H.F.W. Taylor, Proposed structure for calcium silicate hydrate gel, J. Am. Ceram. Soc. 69 (6) (1986) 464–467.
[12] H.F.W. Taylor, Nanostructure of C–S–H: current status, Adv. Cem. Based Mater. 1 (1) (1993) 38–46.
[13] I.G. Richardson, G.W. Groves, Models for the composition and structure of calcium silicate hydrate (C–S–H) gel in hardened tricalcium silicate pastes, Cem. Concr. Res. 22 (6) (1992) 1001–1010.
[14] I.G. Richardson, G.W. Groves, Incorporation of minor and trace elements into calcium silicate hydrate (C–S–H) gel in hardened cement paste, Cem. Concr. Res. 23 (1) (1993) 131–138.
[15] H.F.W. Taylor, Cement Chemistry, Academic Press, London, 1990.
[16] R.K. Iler, The Chemistry of Silica: Solubility, Polymerization, Colloid and Surface Properties, and Biochemistry, Wiley, New York, 1979.